Available online at www.sciencedirect.com
ScienceDirect
Micron 38 (2007) 170–175
micron
www.elsevier.com/locate/micron

Identification of Photosystem I and Photosystem II enriched regions of thylakoid membrane by optical microimaging of cryo-fluorescence emission spectra and of variable fluorescence

F. Vácha [a,b], V. Sarafis [c,d], Z. Benediktyová [a,e], L. Bumba [b,1], J. Valenta [a,f], M. Vácha [g], Ch.-R. Sheue [h], L. Nedbal [a,e,*]

[a] *Institute of Physical Biology, University of South Bohemia, Zámek 136, 37333 Nové Hrady, Czech Republic*
[b] *Biological Centre Academy of Sciences of the Czech Republic, Branišovská 31, 37005 České Budějovice, Czech Republic*
[c] *School of Integrated Biology, University of Queensland, Australia*
[d] *CPFS, University of Western Sydney, Australia*
[e] *Institute of Systems Biology and Ecology, Academy of Sciences of the Czech Republic, Zámek 136, 37333 Nové Hrady, Czech Republic*
[f] *Faculty of Mathematics and Physics, Charles University, Prague, Czech Republic*
[g] *Tokyo Institute of Technology, Tokyo, Japan*
[h] *Institute of Bioresources 1, Hseufu Road, Neipu Pintiung 912, Taiwan*

Abstract

Oxygenic photosynthesis of higher plants requires linear electron transport that is driven by serially operating Photosystem II and Photosystem I reaction centers. It is widely accepted that distribution of these two types of reaction centers in the thylakoid membrane is heterogeneous. Here, we describe two optical microscopic techniques that can be combined to reveal the heterogeneity. By imaging micro-spectroscopy at liquid nitrogen temperature, we resolved the heterogeneity of the chloroplast thylakoid membrane by distinct spectral signatures of fluorescence emitted by the two photosystems. With another microscope, we measured changes in the fluorescence emission yield that are induced by actinic light at room temperature. Fluorescence yield of Photosystem II reaction centers varies strongly with light-induced changes of its photochemical yield. Consequently, application of moderate background irradiance induces changes in the Photosystem II fluorescence yield whereas no such modulation occurs in Photosystem I. This contrasting feature was used to identify regions in thylakoid membranes that are enriched in active Photosystem II.

Keywords: Chloroplast; Heterogeneity; Microscopy; Photosynthesis

1. Introduction

Nearly all forms of life including humans depend on photosynthesis for direct or indirect energy supply. The global relevance of photosynthesis is also in sustaining composition of the Earth atmosphere. Photosynthesis largely mitigates effects of the unprecedented amounts of CO_2 released by our industry. Plants assimilate carbon into biomass and release oxygen back to air. Understanding structure and function of the photosynthetic machinery is required for understanding the very basis of life as well as for increasing our potential to mimic nature and construct artificial photosynthetic systems.

The photosynthetic apparatus is highly conserved in all oxygenic autotrophic organisms—in higher plants, green algae and, to a large extent, also in cyanobacteria (Blankenship, 2002). Solar energy is captured by photosynthetic antennas and transported in forms of excitons to the reaction centers of two types: Photosystem II (PSII) and Photosystem I (PSI). The reaction centers convert the excitonic energy into energy of separated charges in two distinct photochemical reactions that operate in series, driving the electron transport from water on the donor side of PSII to ferredoxin on the acceptor side of PSI (Blankenship, 2002).

Higher plants and green algae are eukaryots with photosynthetic activity concentrated in a specialized organelle—the chloroplast (Staehelin and van der Staay, 1996). The primary photochemical and charge transfer reactions occur in the thylakoid membrane that fills most of the chloroplast volume. Thylakoid is a closed, bag-type membrane system separating

* Corresponding author. Tel.: +420 386361231; fax: +420 386361231.
E-mail address: nedbal@greentech.cz (L. Nedbal).
[1] Present address: Institute of Microbiology, Videnska 1083, 142 20 Prague, Czech Republic.

0968-4328/$ – see front matter © 2006 Elsevier Ltd. All rights reserved.
doi:10.1016/j.micron.2006.07.013

the inner space, lumen, from the outer space, stroma. Topologically it is very complex with regions where several layers of membrane–lumen–membrane–stroma are stacked and closely packed. These regions are called grana. The grana are connected by loose and less densely packed thylakoid regions that are called stroma lamellae.

In spite of the concerted, serial operation of the photosystems, the two types of the reaction centers are not co-localized. Invasive techniques of biochemical separation showed (Anderson and Anderson, 1980; reviewed in Anderson, 2002) that a dominant fraction, ca. 90%, of PSI reaction centers is localized in the stromal regions whereas a dominant fraction, ca. 85%, of PSII centers is found in the granal regions of the thylakoid membrane. This supports the previous electron microscopy freeze-fracture studies on localization of PSI and PSII in thylakoid membrane (for latest reviews on this topic see Staehelin and van der Staay, 1996; Staehelin, 2003)

Recently, non-invasive images of topology of thylakoid membranes were obtained by room temperature confocal microscopy (van Spronsen et al., 1989; Sarafis, 1998; Hepler and Gunning, 1998; Mehta et al., 1999; Gunning and Schwartz, 1999; Osmond et al., 1999). Distribution of photosynthetic complexes in frozen thylakoid was investigated by Vácha et al. (2000, 2006) using scanning confocal microscope with gradient-index lens (Vácha et al., 1999).

Here, we describe two independent microscopic techniques that discriminate between thylakoid segments enriched in PSI and in PSII. Spectral and dynamic features revealed by these techniques are used to map thylakoid domains in isolated intact chloroplasts of *Aglaonema simplex* var. *metallica*.

2. Materials and methods

2.1. Plant material for fluorescence imaging

A. simplex var. *metallica* is a plant found in shade of dense and humid tropical forests of South-East Asia. The plant is known to have a very large and well-structured chloroplast. We grew the plants in shaded glasshouse with photoperiod approximately 12/12 h day/night in pots with garden soil at 26–30 °C, frequently sprayed with water. The pots were in plastic boxes covered with a transparent plastic wrap material to limit evaporation and drying. The incident irradiance was below 10 μmol(photons) m^{-2} s^{-1}. The plants were kept in dark for 24 h prior chloroplast isolation to reduce accumulated starch.

The harvested leaf was chopped by a razor blade in ice-cold isolation medium (0.4 M sucrose, 50 mM Tris/pH 7.5, 10 mM NaCl, 0.1 mM $MgCl_2$) with 1 drop of mercaptoethanol in 500 ml of the medium.

For low-temperature experiments, deep green suspension obtained by chopping the leaf was spread over a cold glass plate separating large debris from suspension containing chloroplasts. The suspension was collected by a Pasteur pipette and centrifuged at 500 × *g* for a minute. Loose pellet from the middle of the cuvette was harvested by Pasteur pipette and resuspended in supernatant obtained by centrifugation of the rest of the suspension at 15,000 × *g* for 15 min. Chloroplasts were diluted in glycerol and cooled in microscope cryostat.

For the room temperature fluorescence measurements the chloroplast suspension was diluted five times in ice-cold resuspension medium (0.33 M Sorbitol, 2 mM EDTA, 1 mM $MgCl_2$, 1 mM $MnCl_2$, 50 mM Hepes–KOH pH 7.6). The chloroplasts were immobilized on a poly-L-lysine coated micro-slide (Ibidi, Germany, http://www.ibidi.com).

2.2. Electron microscopy

A small piece of leaf was washed twice in 50 mM phosphate buffer (pH 7.4) and fixed in a solution containing 2%

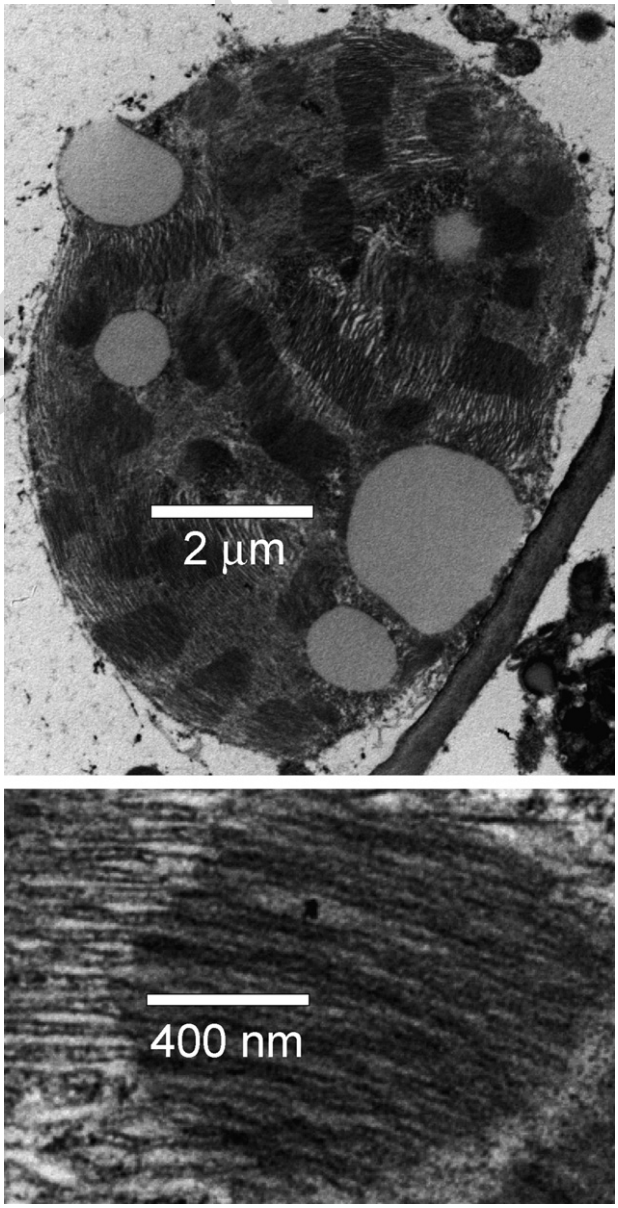

Fig. 1. Top: electron microscopic image of a chloroplast in *Aglaonema simplex* var. *metallica*. The darker, layered structures are the grana. The lighter, more loosely packed interconnected regions are the stroma lamellae. Grayish, homogeneously stained grains is starch. Bottom: a detail showing a granum and adjacent stromal lamellae.

glutaraldehyde in 50 mM phosphate buffer (pH 7.4) for 24 h. This was followed by three washes in phosphate buffer and post-fixated in 1% OsO_4 in 50 mM phosphate buffer (pH 7.4) for 1 h. The cells were again washed three times and the samples were dehydrated in acetone and embedded in Spurr's resin. Thin sections were cut with a diamond knife and post-stained for 30 min with 5% aqueous uranyl acetate followed by lead citrate for 80 s. The images of the leaf ultra-thin sections were obtained with Jeol 1010 electron microscope (Jeol, Tokyo, Japan) equipped with CCD camera MegaView III and image acquisition software analySIS (Soft Imaging Systems, Münster, Germany).

A. simplex var. *metallica* was chosen because its thylakoids are characterised by grana of up to 1.9 μm in diameter (Sarafis, 1998). The top panel in Fig. 1 shows an electron micrograph of a chloroplast cross-section documenting that the thylakoid membrane is structured into dark grana regions and connecting lighter stroma lamellae. A detailed electron microscopy image of a dark granum and of adjacent lighter stroma lamellae is shown in the bottom panel of Fig. 1.

2.3. Cryo-spectrofluorescence microimaging

The cryo-imaging system (Fig. 2) is based on an Olympus IX70 inverted fluorescence microscope with 100 W U-LH100HG mercury lamp as a source of excitation radiation (Olympus, Japan). The long-distance focal plane of the objective (PlanFluorit LCPLFL, 60×, 0.7 N.A., Olympus, Japan) is located inside the optical transmission microcryostat (MMR Technologies, USA) where the chloroplast suspension in 75% glycerol is cooled to 80 K by expanding high-pressure nitrogen. The microscope is equipped with an Olympus U-MSWB filter cube set (Olympus, Japan) containing a 420–480 nm band-pass excitation filter, 515 nm long-pass filter and 500 nm edge dichroic mirror. The chlorophyll fluorescence emission is analyzed spectrally with the imaging spectrometer, Triax 320 (Jobin Yvon-Spex, USA) equipped with two gratings and one mirror on a revolving turret. The images and spectra were detected by the liquid nitrogen-cooled CCD camera with a back-thinned silicon chip (Marconi 42-10; 2048 × 512 pixels, pixel area 13 μm × 13 μm). The camera was attached to the imaging output of the spectrometer.

A broad-spectrum image was first detected with the spectrometer in the mirror position with fully opened entrance slit (7 mm). In the spectral mode, detailed emission spectra of a central image region were measured with a diffraction grating of 300 grooves/mm and the entrance slit closed to 0.5 mm.

Right panel of Fig. 3 shows the image of long-wavelength (>715 nm), 80 K chlorophyll fluorescence emission that is attributed largely to PSI (Satoh, 1979). The short-wavelength fluorescence emission shown by the other gray-scale image (PSII) was calculated as the difference between the total and the long-wavelength emission. The assignment of photosystems to spectrally distinct thylakoid regions is based on the wide consensus attributing the long-wavelength fluorescence emission, 720–740 nm, largely to PSI complexes and the short-wavelength emission, 680–695 nm, largely to PSII complexes (confirmed recently in Vácha et al., 2000). The color image in bottom of Fig. 3 right panel shows the regions of the thylakoid dominated by the long-wavelength emission of PSI (blue) and by the short-wavelength emission of PSII (red). PSII dominates in the high-fluorescence regions of the thylakoid that are, presumably, coinciding with the grana (van Spronsen et al., 1989). The long-wavelength spectral signature of PSI is seen mostly in the complementary stroma lamellae (blue in Fig. 3).

This conclusion was confirmed also by measuring the low-temperature fluorescence emission spectra in the two regions of the thylakoid membrane (left panel in Fig. 3). In the stromal lamellae, the emission spectrum was dominated by the 735 nm band of PSI. The grana emitted mostly the short-wavelength fluorescence with a maximum near 680 nm that is associated with PSII.

2.4. Kinetic chlorophyll fluorescence microscope

In the reaction centers of PSII, the fluorescence quantum yield is inversely proportional to the quantum yield of photochemistry (reviewed in Nedbal and Koblížek, 2006).

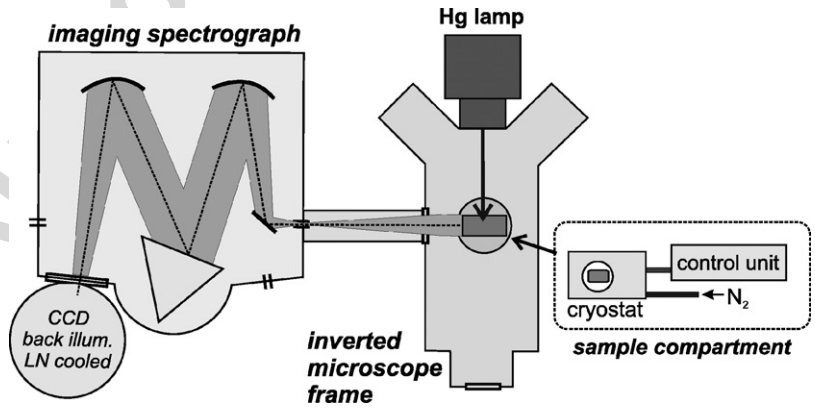

Fig. 2. Cryo-microscope adapted to measure chlorophyll fluorescence emission spectra. The chloroplast suspension between two glass cover slips was kept near liquid nitrogen temperature (77 K) in an optical cryostat mounted on the stage of IX-70 inverted Olympus microscope. The excitation light from a Hg-lamp was focused by a long-working-distance objective (60×, 0.7 N.A.) on the sample. The emitted chlorophyll fluorescence was analyzed by an imaging spectrograph and back-illuminated CCD camera with its chip cooled by liquid nitrogen.

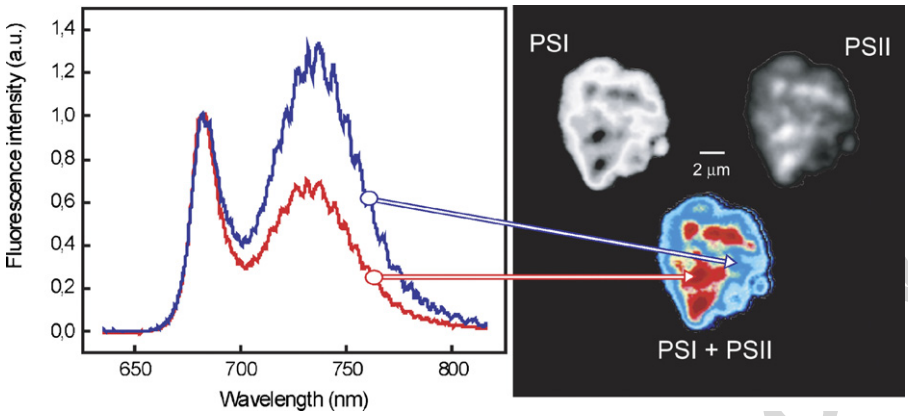

Fig. 3. The two gray-scale images in the right panel show fluorescence emission of the chloroplast in two spectral regions. The PSI fluorescence image was obtained with the blocking filter (RG715). In this mode, the fluorescence emission originated dominantly from PSI ($\lambda_{max} \approx 735$ nm). The PSII image was calculated as a difference between the total chlorophyll fluorescence captured without the blocking filter (not shown) and the PSI image. The color image shows combined PSI-enriched (blue) and PSII-enriched (red) regions of the thylakoid inside the chloroplast. The graphs in the left panel represent 80 K fluorescence emission spectra in the locations shown by the arrows. The red curve shows a spectrum emitted from the high-fluorescence, PSII-enriched region of the thylakoid. The blue curve represents the PSI-enriched region.

The photosynthetic charge transfer pathways are open in a dark-adapted plant leading to the maximal photochemical yield and, consequently, to minimal fluorescence yield (F_0). A strong flash of light can transiently saturate and jam the electron transfer pathways suppressing the photochemical yield to zero and elevating the fluorescence yield to a maximum (F_M). The variable fraction of the fluorescence emission, $F_V = F_M - F_0$, is the kinetic signature of PSII that is widely used for imaging of photosynthetic activity on leaf or plant levels (Nedbal and Whitmarsh, 2004). Several applications of this technique have been already reported on a microscopic scale (Küpper et al., 2000, 2004; Ferimazova et al., 2002). We do not know about any published experimental work aimed at mapping of PSI and PSII activity in isolated chloroplasts with grana and stroma lamellae clearly resolved.

Fig. 4 shows schematically the instrument that we developed to measure the variable part of the chlorophyll fluorescence emission. The optical part of the instrument is based on the inverted IX-70 microscope with 100×, 1.3 N.A. oil-immersion objective UplanApo (http://www.olympus-europa.com/microscopy/, Olympus, Japan). The electronic part is based on the FluorCam imaging system (http://www.psi.cz/, PSI, Czech Republic). Measuring flashes (10 μs, <25 Hz) are generated by a single blue-light emitting diode ($\lambda_{max} \approx 450$ nm, Royal Blue PR09, Lumileds Lighting, LLC, San Jose, CA, USA). The electronic shutter of the FluorCam CCD camera opens only during the measuring flashes (Nedbal et al., 2000). The mean irradiance of the sparse measuring flashes was kept as low as possible so that the photochemical status of the PSII reaction centers and of the electron transport chain remained near to the

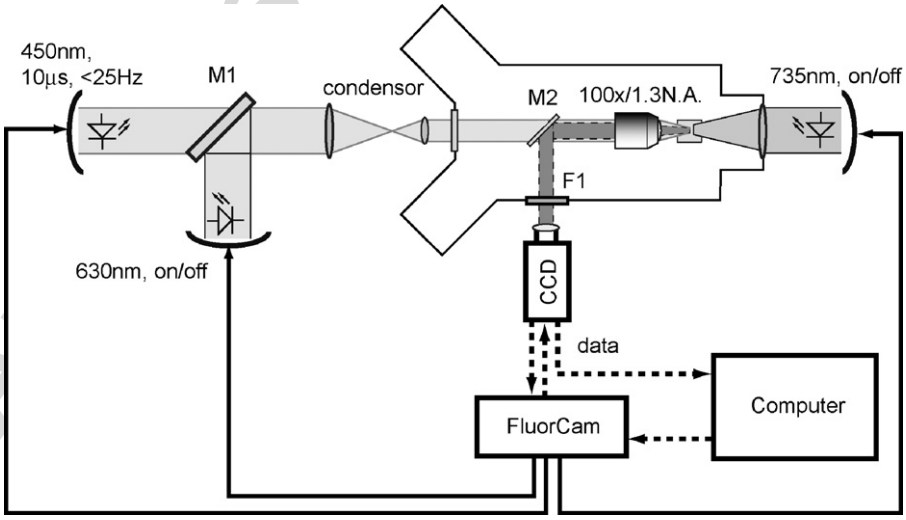

Fig. 4. Kinetic chlorophyll fluorescence microscope consisted of IX-70 microscope (Olympus, Japan) and of FluorCam imaging system (PSI, Czech Republic). The measuring light to excite fluorescence ($\lambda_{max} \approx 450$ nm), the light oxidizing the acceptor side of PSII ($\lambda_{max} \approx 735$ nm) and the light transiently reducing the acceptor side of PSII ($\lambda_{max} \approx 630$ nm) were generated by light emitting diodes controlled and power-supplied by FluorCam. The Lumiled diodes were placed in 2° mirror collimators (Roithner, Vienna, Austria). The electronic shutter of the CCD camera was synchronized with the measuring flashes to minimize offset due to background and actinic light signals.

dark-adapted state (F_0). This condition is relatively easy to satisfy with low magnification objectives that yield images with the F_V/F_M ratio of 0.8, identical to levels observed in intact leaves. It is much harder to reach the high F_V/F_M with high-magnification objectives used here because the photon-flux density yielding satisfactory signal levels is too high to avoid some actinic effects. The actinic effects of the measuring light can be reduced by continuous background illumination by far-red light that selectively drives PSI ($\lambda_{max} \approx 740$ nm, LED740-66-60, Roithner Lasertechnik, Vienna, Austria). The far-red irradiance was applied to the sample from the side opposite to the objective for 1 s prior the F_0 measurement.

The maximum chlorophyll fluorescence yield, F_M was measured during 1 s-long, saturating irradiance exposure to light from the Lumiled PD01 diode source ($\lambda_{max} \approx 630$ nm, Lumileds Lighting, LLC, San Jose, CA, USA). The flashing measuring light (450 nm) and the saturating light (5000 μmol(photons) m^{-2} s^{-1}, 630 nm) were combined by a dichroic mirror M1 ($\lambda_{edge} \approx 520$ nm, PSI, Brno, Czech Republic).

Chlorophyll fluorescence was diverted towards the CCD camera by the dichroic mirror M2 ($\lambda_{edge} \approx 640$ nm, PSI, Brno, Czech Republic) that transmitted the measuring flashes as well as the saturating light. There was an RG 695 red-edge filter in front of the CCD chip.

The instrument was recording full Kautsky effect transients in each pixel capturing chlorophyll fluorescence (Nedbal and Whitmarsh, 2004). The maximum time resolution was 40 ms with approximate determination of F_0 achieved as described above. The transients did not prove any substantial heterogeneity in the fluorescence rise kinetics probably because of high noise levels of non-averaged signals (not shown).

Fig. 5 shows images of chlorophyll fluorescence emission of three isolated chloroplasts at room temperature. The F_M (top left) and approximate F_0 (top right) images reveal the granal structure within the chloroplast. The grana are visualized as the bright regions with high chlorophyll fluorescence. The variable fluorescence $F_V = F_M - F_0$ originating from PSII is mapped in the bottom left panel in an image resembling qualitatively the top row images of F_M and F_0. Assuming that the F_0 signal is approximately reflecting the density of the fluorescence emitting chlorophyll, we propose that the ratio F_V/F_0 image shown in the bottom right panel of Fig. 5 maps the relative distribution of active PSII reaction centers. The chloroplasts 1 and 2 show no granal structure in the relative distribution of active PSII. The F_V/F_0 image of the chloroplast 3 indicates a high PSII activity in the grana and low PSII activity in the stroma lamellae. We assume that the chloroplasts 1 and 2 were partially disrupted with scrambled organization of the thylakoid membrane whereas the chloroplast 3 was intact with preserved natural structure of the thylakoid.

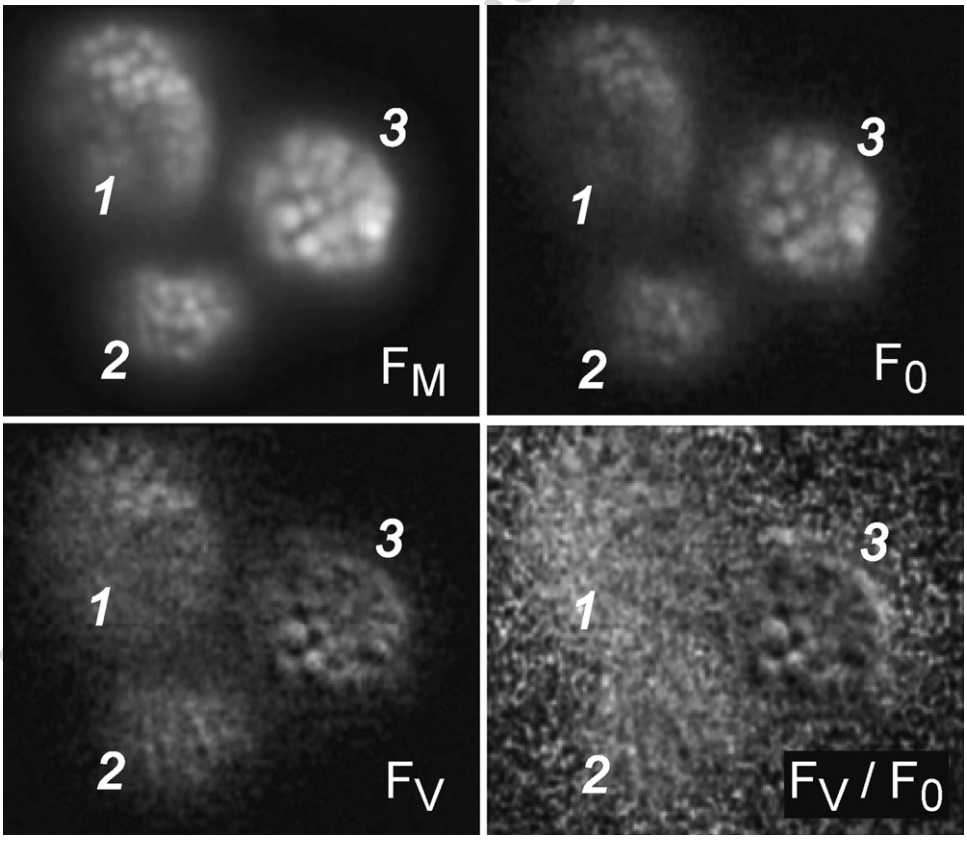

Fig. 5. Images of room temperature, chlorophyll fluorescence emission F_M (top left) and approximate F_0 (top right) of three isolated chloroplasts. The bottom left panel shows the variable fluorescence, the difference $F_V = F_M - F_0$. The variable fluorescence originates from the light-induced changes of photochemical yield that are specific to PSII. The bottom right panel shows the variable fluorescence normalized to the minimal fluorescence. The gray scale of F_M, F_0 and of F_V images is uniform with black corresponding to 0 signal and white to the relative signal of 255. The ratio F_V/F_0 is renormalized to its minimum at 0 and maximum at 255.

3. Discussion

We report construction of two instruments for mapping of PSI and PSII distribution and activity in native chloroplasts. Resolution of individual grana and stroma lamellae regions in the chloroplast thylakoid was demonstrated using both methods—with the fluorescence microscopy resolving the low-temperature emission spectra and with the kinetic fluorescence microscopy resolving variable fluorescence emitted from PSII. The experiments showed that both techniques are capable of detecting high concentration of PSII in the grana and high concentration of PSI in the stroma lamellae. This result is relevant because it opens up the possibility of monitoring the distribution of the two photosystems non-invasively in native systems. We ascribe the differences in size and shape of chloroplast and, in particular, of grana in low and room temperature fluorescence images (Figs. 3 and 5) to the changes caused by slow freezing of the chloroplasts in Fig. 3. The kinetic chlorophyll fluorescence microimaging can monitor dynamics of the photosynthetic apparatus in real time while resolving details of the thylakoid organization. Two major improvements are needed to maximize the impact of the technique—chloroplasts have to be imaged in a highly active physiological state with a further decreased photon-flux density of the measuring flashes. The typical F_V/F_0 ratio of an intact chloroplast should be 4–5 while, here, we achieved typical a ratio of 1. With the higher signal/noise ratio it will be rewarding to image the thylakoid regions with distinct spectral features (Oijen et al., 1998) as well as the PSII activity in three-dimensions. Spectral resolution beyond the classical limit is feasible also in the third dimension and is favored by higher apertures since the cross-talk between the spectrally distinct emitters is minimized.

With these improvements, the dynamics of photosynthetic apparatus and, in particular, the dynamics of the PSII heterogeneity within a native thylakoid membrane (Lavergne and Briantais, 2002) will become directly accessible. The role of grana in photosynthesis remains unresolved, largely as a result of the lack of microscopic resolution of the processes involved. Achieving this goal will provide a means to solve one of the great puzzles of photosynthesis.

Acknowledgements

We thank Ruth Kiew for helping with the provision of *A. simplex* var *metallica*. The research was supported in part by the grants of the Ministry of Education, Youth and Sports of the Czech Republic MSM 6007665808 (FV, ZB, JV, LN), MSM0021620835 (JV), and FRVS 3243/2005 (ZB), grants of the Academy of Sciences of the Czech Republic AV0Z60870520 (ZB, LN), AV0Z50510513 (FV, LB), AV0Z5020903 and by the grant of the Grant Agency of the Czech Republic GACR 206/05/0894 (LN).

References

Anderson, B., Anderson, J.M., 1980. Lateral heterogeneity in the distribution of chlorophyll–protein complexes of the thylakoid membranes of spinach chloroplasts. Biochim. Biophys. Acta 593, 427–440.

Anderson, J.M., 2002. Changing concepts about the distribution of Photosystems I and II between grana-appressed and stroma-exposed thylakoid membranes. Photosynth. Res. 73, 157–164.

Blankenship, R.E. (Ed.), 2002. Molecular Mechanisms of Photosynthesis. Blackwell Science Ltd., Oxford.

Ferimazova, N., Küpper, H., Nedbal, L., Trtílek, M., 2002. New insights into photosynthetic oscillations revealed by two-dimensional microscopic measurements of chlorophyll fluorescence kinetics in intact leaves and isolated protoplasts. Photochem. Photobiol. 76 (5), 501–508.

Gunning, B.E.S., Schwartz, O.M., 1999. Confocal microscopy of thylakoid autofluorescence in relation to origin of grana and phylogeny in the green algae. Aust. J. Plant Physiol. 26, 695–708.

Hepler, P.K., Gunning, B.E.S., 1998. Confocal fluorescence microscopy of plant cells. Protoplasma 201, 121–157.

Küpper, H., Šetlík, I., Trtílek, M., Nedbal, L., 2000. A microscope for two-dimensional measurements of *in vivo* chlorophyll fluorescence kinetics using pulsed measuring light, continuous actinic light and saturating flashes. Photosynthetica 38 (4), 553–570.

Küpper, H., Ferimazova, N., Šetlík, I., Berman-Frank, I., 2004. Traffic lights in *Trichodesmium*. Regulation of photosynthesis for nitrogen fixation studied by chlorophyll fluorescence kinetic microscopy. Plant Physiol. 135 (4), 2120–2133.

Lavergne, J., Briantais, J.-M., 2002. Photosystem II heterogeneity. In: Ort, D.R., Yocum, C. (Eds.), Oxygenic Photosynthesis: The Light Reaction. Kluwer Academic Publishers, Dordrecht, pp. 11–30.

Mehta, M., Sarafis, V., Critchley, C.C., 1999. Thylakoid membrane architecture. Aust. J. Plant Physiol. 26, 709–716.

Nedbal, L., Koblížek, M., 2006. Chlorophyll fluorescence as a reporter on in vivo electron transport and regulation in plants. In: Grimm, B., Porra, R., Rüdiger, W., Scheer, H. (Eds.), Biochemistry and Biophysics of Chlorophylls. Springer-Verlag, Dordrecht.

Nedbal, L., Soukupová, J., Kaftan, D., Whitmarsh, J., Trtílek, M., 2000. Kinetic imaging of chlorophyll fluorescence using modulated light. Photosynth. Res. 66, 3–12.

Nedbal, L., Whitmarsh, J., 2004. Chlorophyll fluorescence imaging of leaves. In: Govindjee, Papageorgiou, G. (Eds.), Chlorophyll Fluorescence: A Signature of Photosyntesis. Springer-Verlag, Dordrecht, pp. 389–407.

Oijen, A.M., Köhler, D.K., Schmidt, J., Müller, M., Brakenhoff, G.J., 1998. 3-Dimensional superresolution by spectrally selective imaging. Chem. Phys. Lett. 292, 183–187.

Osmond, B., Schwartz, O., Gunning, B., 1999. Photoinhibitory printing on leaves, visualised by chlorophyll fluorescence imaging and confocal microscopy, is due to diminished fluorescence from grana. Aust. J. Plant Physiol. 26, 717–724.

Sarafis, V., 1998. Chloroplasts: a structural approach. J. Plant Physiol. 152, 248–264.

Satoh, K., 1979. Properties of light-harvesting chlorophyll *a*/*b*protein, and Photosystem I chlorophyll *a*-protein, purified from digitonin extracts of spinach chloroplasts by isoelectrofocusing. Plant Cell Physiol. 20, 499–512.

Staehelin, L.A., van der Staay, G.W.M., 1996. Structure, composition, functional organization and dynamic properties of thylakoid membranes. In: Ort, D.R., Yocum, C. (Eds.), Oxygenic Photosynthesis: The Light Reaction. Kluwer Academic Publishers, Dordrecht, pp. 11–30.

Staehelin, L.A., 2003. Chloroplast structure: from chlorophyll granules to supra-molecular architecture of thylakoid membranes. Photosynth. Res. 76, 185–196.

Vácha, F., Vácha, M., Bumba, L., Hashizume, K., Tani, T., 2000. Inner structure of intact chloroplasts observed by a low temperature laser scanning microscope. Photosynthetica 38 (4), 493–496.

Vácha, F., Adamec, F., Valenta, J., Vácha, M., 2006. Spatial location of photosystem pigment-protein complexes in thylakoid membranes of chloroplasts of *Pisum sativum* studied by chlorophyll fluorescence. J. Lumin., in press.

Vácha, M., Yokoyama, H., Tokizaki, T., Furuki, M., Tani, T., 1999. Laser scanning microscope for low temperature single molecule and micro-scale spectroscopy based on gradient index optics. Rev. Sci. Instrum. 70 (4), 2041–2045.

van Spronsen, E.A., Sarafis, V., Brakenhoff, G.J., van der Voort, H.T.M, Nanninga, N., 1989. 3-Dimensional structure of living chloroplasts as visualized by confocal scanning laser microscopy. Protoplasma 148, 8–14.